Journal of the Korean Vacuum Society
Vol. 3, No. 4, December 1994, pp. 426-433

Characteristics of Oxide Films Deposited with Remote Plasma Enhanced Chemical Vapor Deposition at Low Temperatures From SiH_4-N_2O

Jin-Kyu Kang*, Young-Bae Park and Shi-Woo Rhee

Laboratory for Advanced Materials Processing(LAMP)
Dep't of Chemical Engineering Pohang University of Science and Technology(POSTECH) Pohang, 790-784, Korea
(Received August 22, 1994)

원거리 플라즈마 화학증착에 의한 실리콘 산화막의 물성

강진규 · 박영배 · 이시우

포항공과대학교 화학공학과 재료공정연구실
(1994년 8월 22일 접수)

Abstract – SiH_4-N_2O was used to deposit SiO_2 on Si at low temperatures between room temperature and up to 350℃ in a remote plasma enhanced chemical vapor deposition reactor. It was found out that the effect of plasma power, reactant gas composition and the deposition temperature was quite significant on the chemical composition and structure of the oxide films and also electrical properties of SiO_2 and Si and SiO_2 interface. Too much plasma power and higher ratio of N_2O/SiH_4 degraded oxide and interface properties due to the impurity incorporation and powder formation.

요 약 – 원거리 플라즈마 화학증착 반응기에서 SiH_4-N_2O로 부터 산화막을 증착하고 막의 화학적 조성, 구조, 전기적인 특성 등을 평가하였다. 증착온도는 실온에서 350℃ 사이의 저온이었다. 증착온도, 플라즈마 전력, 반응기체의 조성 등이 막의 물성에 영향을 주는 것으로 나타났으며 나아가서는 산화막과 규소-산화막 계면의 전기적인 특성에도 영향을 주었다. 높은 전력 및 SiH_4-N_2O비에서 막의 물성이 나빠지는 것으로 나타났으며 이 경우 막의 불순물 함량이 높고 또한 기상에서 입자가 형성되는 것이 관찰되었다.

1. Introduction

There is presently much interest in growing silicon oxide films at low temperatures in integrated circuit processing [1-6] Low temperature deposition of dielectric films are usually required for passivation and isolation layers, and also gate insulators for applications such as thin film transistors (TFT). In particular, in the field of active matrix liquid crystal display, the use of oxides along with silicon films deposited at low temperatures is desirable to utilize low cost glass substrates [7, 8]. At low temperatures, it is relatively difficult to grow good films because adatom mobility is low and incorporation of impurities is more likely.

This reduction in deposition temperature, in most cases, degraded electrical performance of the devices and it is required to develop a low temperature process which can give acceptable material properties. The low temperature silicon oxide films can be deposited by methods such as PECVD [9], Photo-CVD [10], and ECR plasma CVD [11]. Usually low temperature oxide property was inferior to thermal oxides because of the incorporation of hydrogen related impurities, such as Si-H, Si-OH, and

*now at Lucky-Goldstar R&D Complex, Anyang, Korea

H_2O [3].

Remote plasma chemical vapor deposition (RPCVD) was also used for silicon oxide film deposition [12, 13]. The RPCVD reactor is mainly separated into two regions. One is upstream region where the plasma is generated, and the other is downstream region where solid materials are deposited without plasma damage. By introducing each reactant gas either into the plasma zone or downstream of the plasma, reaction pathways can be adjusted to minimize the impurity incorporation by avoiding unwanted chemical reactions. Reaction mechanism of SiO_2 deposition has been studied by many researchers [13-20]. Cobianu *et al.* [14] showed that the deposition rate had an increase-maximum-decrease dependence with the increasing oxygen to silane ratio and explained this dependence with Langmuir-Hinshelwood surface reaction theory. At higher ratio of O_2/SiH_4, they pointed out that oxygen coverage on the surface inhibited the adsorption of silane and thus the deposition rate decreased. They, however, did not consider the possibility of gas phase nucleation. Taft [17] suggested that this increase-maximum-decrease dependence was due to the gas phase powder formation at high oxygen to silane ratio and in this case, reactants were consumed in the gas phase and flowed out of the reactor. Recently, it was suggested that the precursor of SiO_2 films is formed in the gas phase [18-20] and the precursor in the gas phase was suggested to be silanol (H_3SiOH) or disiloxane (Si_2H_6O) although the detailed reaction mechanism has not been clarified. They, however, did not point out the effect of gas phase reactions on the powder formation and film properties. Joyce *et al.* [21] studied the effect of N_2O/SiH_4 ratio and deposition temperature on the film properties, especially the etch rate. They pointed out that films deposited at low temperatures and with higher N_2O/SiH_4 ratio had higher etch rate. It was generally known that less dense films with impurities and pin holes showed higher etch rate and this was true for films deposited at low temperatures. The purpose of the present study was to investigate the effect of the operating variables, such as deposition temperature, plasma power and especially partial pressure ratio of reactants (N_2O

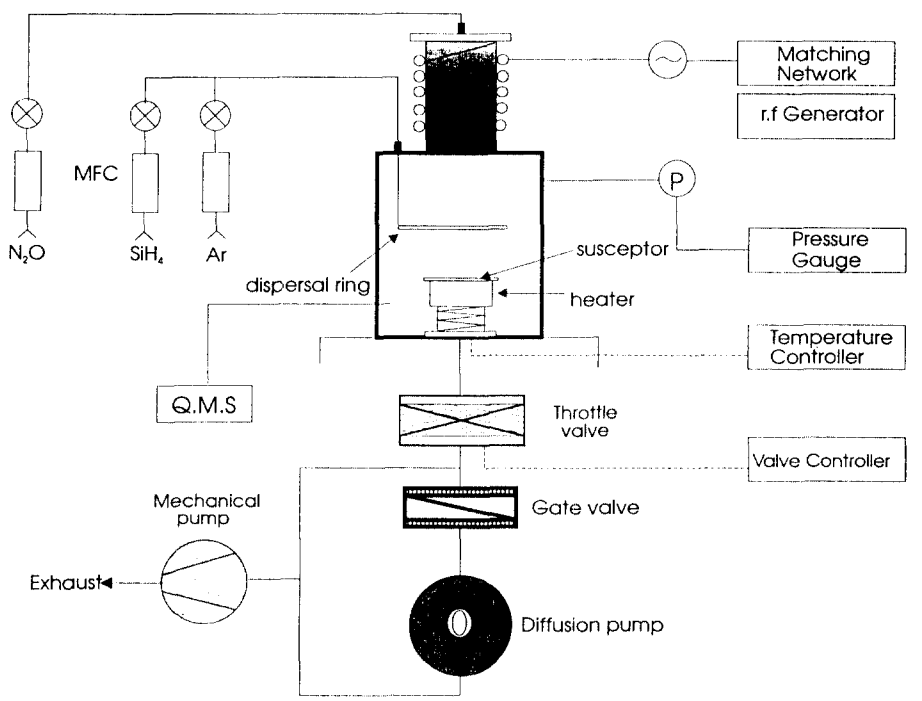

Fig. 1. Schematic diagram of the experimental setup for remote plasma chemical vapor deposition.

/SiH_4 ratio) on the material properties of the silicon oxide films deposited in a remote plasma CVD reactor.

2. Experiment

A remote plasma enhanced CVD reactor system with inductively coupled plasma, as shown in Fig. 1 was used. A coil was wound around the quartz tube that was 7.5 cm in diameter and 20 cm in length. N_2O (99.9995%) was introduced into the quartz tube and excited by 13.56 MHz plasma to produce activated oxygen radical and flowed into the deposition zone. Silane (99.99%) mixed with argon was introduced into the region 10 cm downstream of the plasma and mixed with excited oxygen and flowed toward the substrate 20 cm down stream of the plasma. P-type 4 inch silicon wafer with 〈111〉 orientation was used as a substrate. The base pressure was 2×10^{-6} torr maintained by diffusion pump, reactor pressure was at 400 mtorr during the deposition, deposition temperatures were 25~350℃, SiH_4 flow rate was 3 sccm, N_2O flow rate was 3~36 sccm and plasma power was 15~100 watts. Total flow rate was fixed at 70 sccm by adjusting argon flow rate. Modified RCA method was used for the pre-deposition cleaning and the substrate was pre-baked for 30 min to eliminate the moisture. Deposited films were characterized by FT-IR and ESCA for chemical composition, ellipsometry for refractive index and film thickness, electron spin resonance (ESR) for the amount of dangling bonds and I-V and C-V characteristics for electric properties.

3. Results and Discussion

Fig. 2 shows the deposition rate as a function of the deposition temperature at various plasma powers. The deposition rate is more sensitive on the plasma power than on the substrate temperature and becomes saturated at high plasma power. The activation energy is about 1.2~3.2 kcal/mole which is much smaller than 41~45 kcal/mole in case of thermal CVD.

Fig. 3 shows FT-IR spectra representing the effect

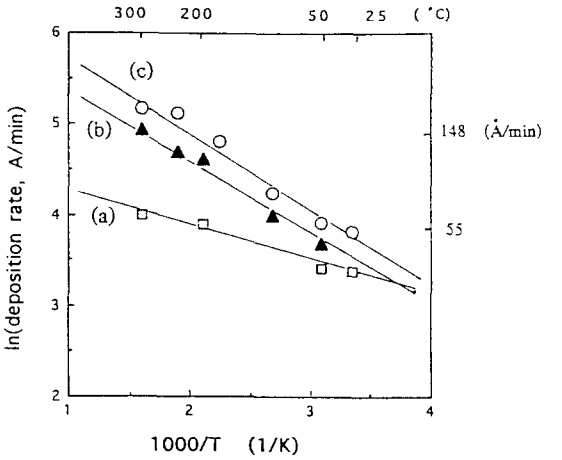

Fig. 2. Arrhenius plot for temperature dependence of the deposition rate with pressure at mtorr, $N_2O/SiH_4/Ar=12/3/55$ sccm, plasma power at (a), 15W, (b) 50W, (c) 100W

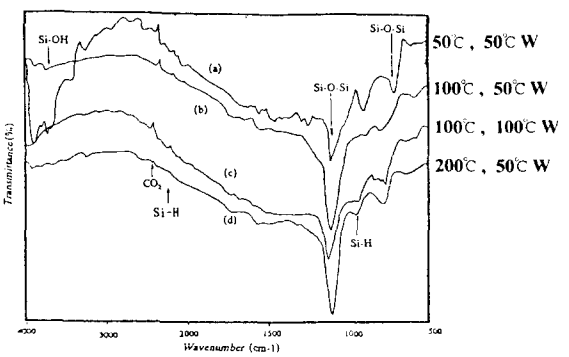

Fig. 3. FT-IR spectra of oxide films with $N_2O/SiH_4/Ar=12/3/55$ sccm
(a) T=50℃, plasma power 50W (b) T=100℃, plasma power 50W
(c) T=100℃, plasma power 100W (d) T=200℃, plasma power 50W

of deposition temperature on the chemical composition of the oxide films. Si-OH usually appears in the range of 3605~3150 cm^{-1} and 930~950 cm^{-1}, and Si-H at around 2260~2280 cm^{-1} and 880~860 cm^{-1}, Si-O at around 1040~1080 cm^{-1} and 800~815 cm^{-1} [22]. Films deposited at low temperatures contain larger amount of Si-OH and Si-H and this is probably due to the reaction with water vapor. At higher temperatures, byproduct water vapor will

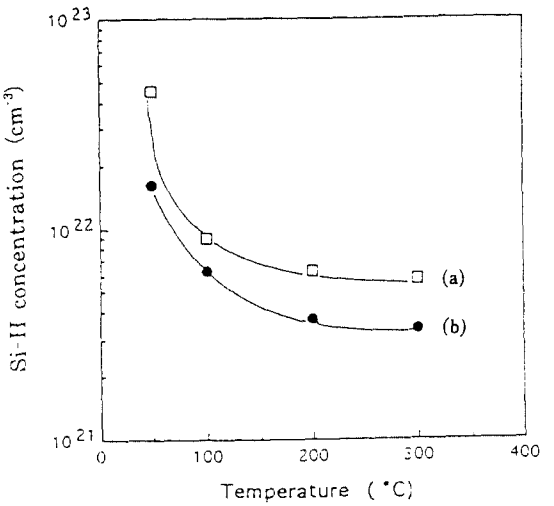

Fig. 4. Effect of deposition temperature on the concentration of Si-H bond in oxide films. $N_2O/SiH_4/Ar=12/3/55$ sccm, and (a) 100W, (b) 50W.

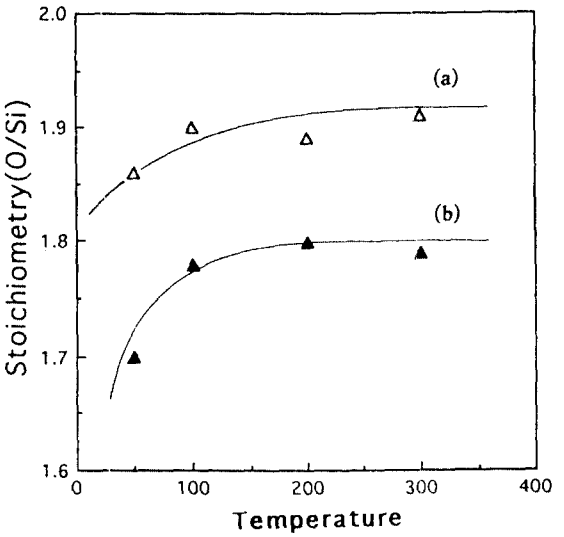

Fig. 5. Effect of the deposition temperature on the film stoichiometry (O/Si) of oxide films with $N_2O/SiH_4/Ar=12/3/55$ sccm and (a) 50W, (b) 100W plasma power.

be evaporated from the surface. The amount of Si-H bond incorporated in the film can be calculated from Si-H stretching peak around 2260~2280 cm^{-1} to estimate the Si-H concentration as shown in Fig. 4. This Si-H can be as high as 10% especially at low deposition temperatures.

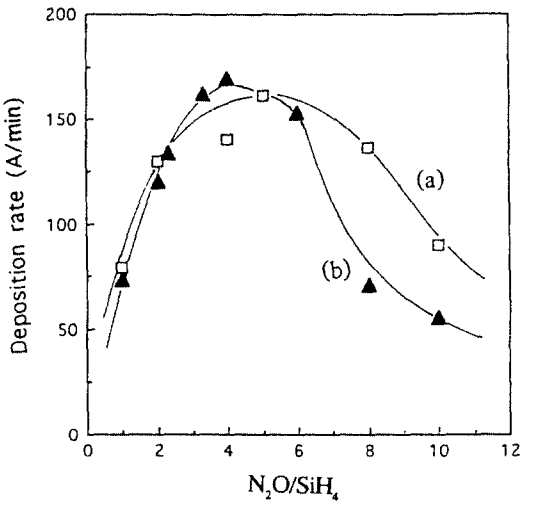

Fig. 6. Effect of the N_2O/SiH_4 ratio on the deposition rate of oxide films. T=200℃, SiH_4=3 sccm, $N_2O+Ar=67$ sccm and (a) 50W, (b) 100W plasma power

The film stoichiometry (O/Si ratio) was analyzed with ESCA composition analysis and is shown in Fig. 5. The ratio becomes smaller at low temperatures and at higher plasma powers probably due to the incorporation of Si-H, -OH and Si-OH.

Fig. 6 shows the effect of N_2O/SiH_4 ratio on the deposition rate with plasma power of 50 and 100 watts. At reactant ratio of about 4, the deposition rate was highest and decreases at higher ratio. The formation of powder was observed at higher ratio of N_2O/SiH_4 and it is believed that powders formed in the gas phase are carried out of the reactor and the deposition rate becomes smaller. This tendency appears stronger with higher plasma power. The TEM micrograph of powders collected on the TEM grid placed inside the reactor during the deposition is shown in Fig. 7. The size of the powder is in the range of 0.05~0.1 microns and they are amorphous. The particles formed in the CVD process usually leads to the formation of poor quality films and causes reliability problems in the integrated circuit processing.

Fig. 8 shows the etch rate of oxide films formed with various N_2O/SiH_4 ratios in the buffered HF solution. It can be seen that films deposited at N_2O/SiH_4 of about 4 gives highest density and films formed at N_2O/SiH_4 greater than 4 are less dense

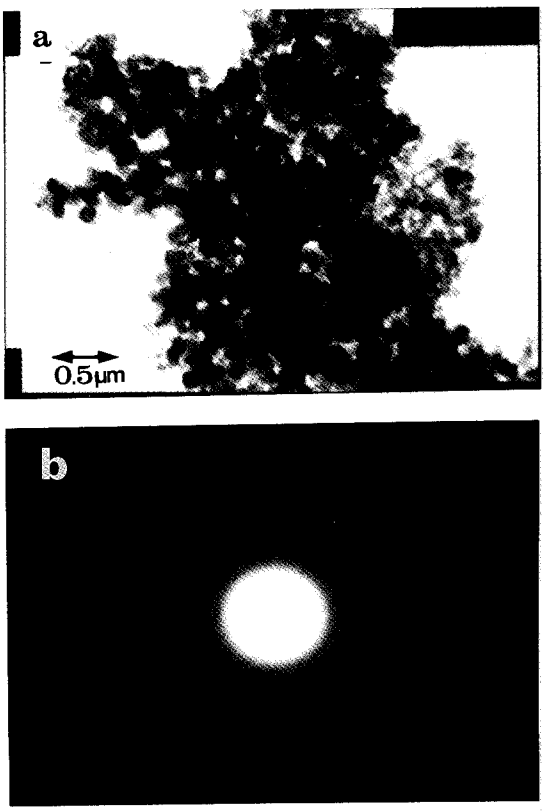

Fig. 7. TEM micrograph of powders collected in the reactor during the deposition, a) size and shape, b) diffraction pattern. T=200℃, SiH_4=3 sccm, N_2O=24 sccm and 50W plasma power.

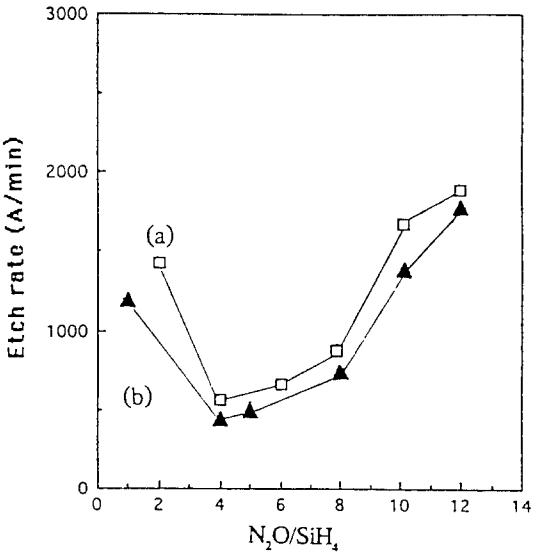

Fig. 8. Effect of the N_2O/SiH_4 ratio on the etch rate of oxide films in buffered HF solution. T=200 ℃, SiH_4=3 sccm, N_2O+Ar=67 sccm and (a) 50W, (b) 100W plasma power.

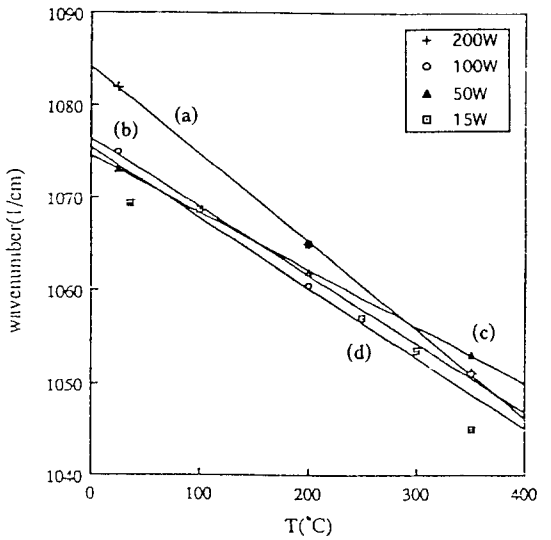

Fig. 9. Effect of the deposition temperature on the stretching wave number of oxide films, a) 200W, b) 100W, c) 50W, d) 15W plasma power, N_2O/SiH_4=4.

because of the powder formation in the gas phase. And also films formed at N_2O/SiH_4 smaller than 4 are silicon rich because of the oxygen deficiency in the film. Silicon rich films show higher etch rate in HF solution.

Fig. 9 shows the wave number of Si-O-Si stretching peak observed in the FT-IR spectrum. This wave number gives the bond angle of Si-O-Si, *i.e.*, U=1134 sin(A/2) where A is bond angle and U is wave number [1]. Also the full width of the peak at half maximum gives the distribution of the bond angle. Films deposited at low temperatures show wider bond angle because the film is porous and films deposited at high temperatures show smaller angle because of the stress from the mismatch of thermal expansion coefficient differnece of Si substrate and growning oxide. Upon annealing, oxide films show wave number of 1063 cm^{-1}, which is close to thermal oxides, regardless of deposition temperature. Also the films deposited with powder formation shows wider bond angle distribution.

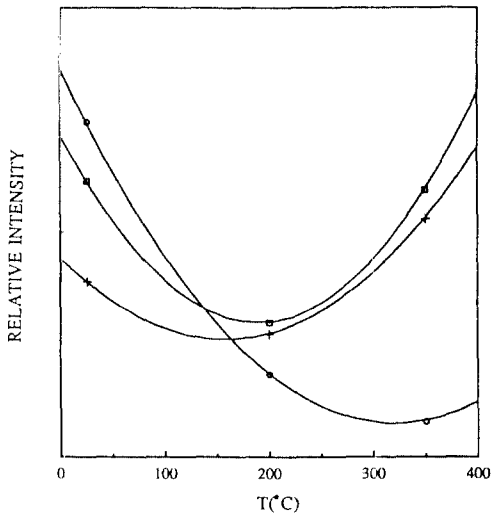

Fig. 10. Effect of the deposition temperature on the ESR peak intensity of oxide films
□: 15W, +: 50W, ○: 100W plasma power, $N_2O/SiH_4=4$.

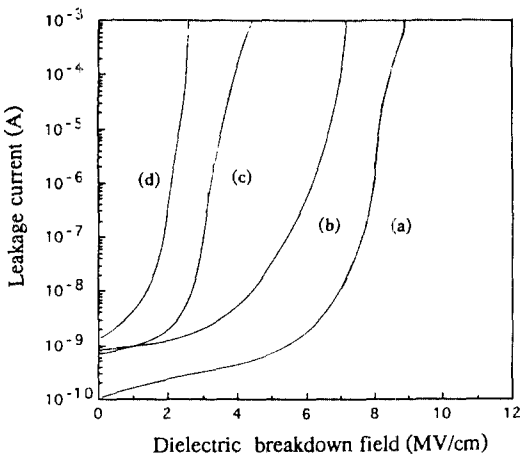

Fig. 11. Current-voltage characteristics of oxide films (a) thermal oxide, (b) $N_2O/SiH_4/Ar=12/3/55$ sccm, 50W, (c) $N_2O/SiH_4/Ar=12/3/55$ sccm, 100W, (d) $N_2O/SiH_4/Ar=24/3/43$ sccm, 10W.

Fig. 10 shows the relative intensity of ESR peak for SiO_2 on Si substrate. The peak appeared at $g=2.0056$ which corresponds to the Pb center from Si dangling bonds at the SiO_2-Si interface. The peak intensity represents the concentration of Si dangling bonds, and at low and high temperatures, the peak intensity becomes higher with minimum at around 200℃. At low temperatures, the films are porous

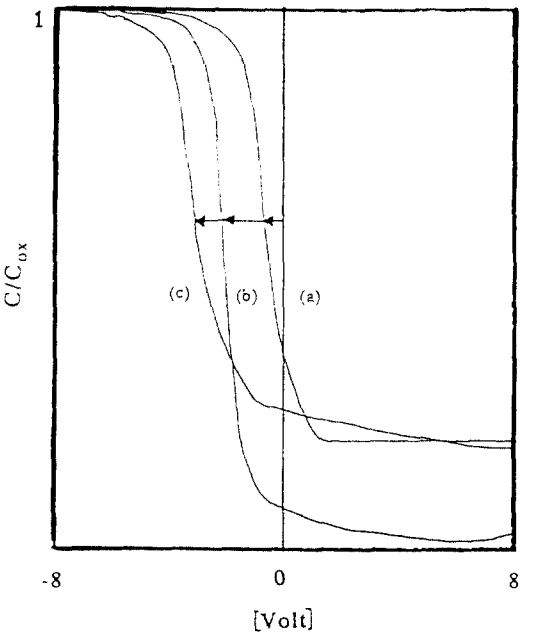

Fig. 12. Capacitance-voltage characteristics in the high frequency (1 MHz) range.
(a) thermal oxide (flat band shift = −0.9 V), (b) $N_2O/SiH_4/Ar=12/3/55$ sccm, 50W (flat band shift = −1.9 V), (c) $N_2O/SiH_4/Ar=12/3/55$ sccm, 100W (flat band shift = −2.27 V).

with higher impurity concentrations and there seems to be more defects at the interface. At high temperatures, stress induced defects are likely to be formed at the interface. With powder formations, peak intensity is higher due to the lack of passivation effect of Si dangling bonds at the interface during the deposition.

Fig. 11 shows the current-voltage (I-V) characteristics of oxide films on Si wafer measured from MOS capacitor made by depositing aluminum as an electrode on top of SiO_2 and bottom of Si wafer and thermal oxide film is compared with plasma oxide deposited in this study. The leakage current increases through the oxide film which was deposited with impurity incorporation at low deposition temperature, gas phase powder formations and too much plasma power. Especially when N_2O/SiH_4 ratio was 8, the breakdown voltage, defined by leakage current above 10^{-6} A, and leakage current are ~2 MV/cm and the order of 10^{-8} A, respectively. Because the film is porous with pinholes and high im-

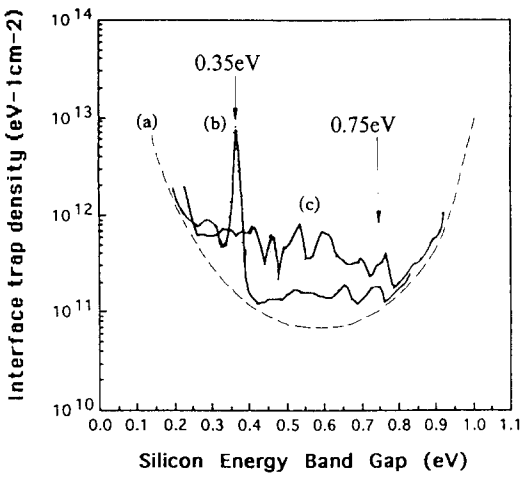

Fig. 13. Interface trap density distribution in the silicon band gap calculated by Terman method from capacitance-voltage data in the high frequency range.
(a) ideal curve, (b) 100W, (c) 50W

purity concentration due to the powder formation.

Fig. 12 shows capacitance-voltage (C-V) measurements and it can be seen that flat band voltage shift moves more towards negative value with oxide films deposited with higher plasma power because the oxide fixed charge increases. With powder for mations at high N_2O/SiH_4 ratio, flat band voltage shift was bigger.

From high frequency C-V measurements, interface trap density (D_{it}) can be calculate as a function of the silicon band gap energy state of silicon energy band gap (1.1 eV) and the results are shown in Fig. 13. For an ideal case, the distribution is like an U shape continuum as shown in dotted line (a). The conventional required interface trap density level is $1\sim2\times10^{11}/eVcm^2$ at the midgap in case of SiO_2 deposited on Si (111) plane [24]. As the concentration of interface trap density between 0.3~0.35 eV which reported as P_b center [25] in case of Si (111) plane increases, we get a peak in the silicon energy band gap energy state above 0.3~0.35 eV and 0.75 eV from the valence band edge as shown in (b) and (c). This peak was observed due to the P_b center from silicon dangling bond as reported by Poindexter, *et al.* [25].

4. Conclusions

Low temperature CVD oxide films were deposited in a remote plasma enhanced chemical vapor deposition reactor from N_2O and SiH_4 and deposition rate, and material properties like chemical composition, Si-O-Si bond angle, etch rate and dangling bond concentrations were measured. Also the electrical properties like I-V and C-V characteristics were measured. It was shown that operating variables like plasma power, deposition temperature and reactant concentrations have a significant effect on the material properties and electrical properties. To make a good material suitable for electronic devices, the relations between process parameters, material properties, and electrical properties should be elucidated comprehensively.

Acknowledgment

This research was supported by Lucky-Gold Star Co.

References

1. G. Lucovsky, S. S. Kim and J. T. Fitch, *J. Vac. Sci. Technol.*, **B8**(4), 822 (1990).
2. G. Lucovsky, J. T. Fitch, D. V. Tsu and S. S. Kim, *J. Vac. Sci. Technol.*, **A7**(3), 1136 (1989).
3. S. S. Kim, D. J. Stephens, G. Lucovsky, G. G. Fountain and R. J. Markunas, *J. Vac. Sci. Technol.*, **A8**(3), 2039 (1990).
4. P. Balk, The Si-SiO_2 System, Elsivier, p. 85 (1986).
5. F. J. Hinpsel, A. Taleb-Ibrahimi and J. A. Yarunouff, The Physics and Chemistry of Si-SiO_2 Interfaces, Plenum Press, N. Y. (1988).
6. H. M. Dauplaise, K. Vaccaro, B. R. Bennett, and J. P. Lorenzo, *J. Electrochem. Soc.*, **9**(6), 1684 (1992).
7. Il-Jeong Lee, Shi-Woo Rhee and Sang Heup Moon, *Appl. Phys. Lett.*, submitted, (1994).
8. Young-Bae Park, Jin-Kyu Kang and Shi-Woo Rhee, *Appl. Phys. Lett.*, submitted, (1994).
9. A. C. Adams, F. R. Alexander, C. D. Capio, and T. E. Smith, *J. Electrochem.Soc.*, **128**, 1545 (1981).
10. S. Szikora, W. Krauter, and D. Bauerle, *Mater. Lett.*, **2**, 263 (1984).
11. S. Matsuo, and M. Kiuchi, Jpn. *J.Appl. Phys.*, **22**,

L210 (1983).
12. G. Lucovsky, D. V. Tsu, *J. Vac.Sci. Technol.*, **A5**(4), 2231 (1987).
13. L. G. Meiners, *J. Vac.Sci. Technol.*, **21**, 655 (1982).
14. C. Cobianu and C. Pavelescu, *Thin Solid Films*, **117**, 211 (1984).
15. C. Cobianu and C. Pavelescu, *Thin Solid Films*, **102**, 36 (1983).
16. B. J. Baliga and S. K. Ghandhi, *J. Appl. Phys.*, **44**, 990 (1973).
17. E. A. Taft, *J. Electrochem. Soc.*, **126**, 1728 (1979).
18. K. Watanabe and H. Komiyama, *J. Electrochem. Soc.*, **137**, 1222 (1990).
19. T. Kawahara, A. Yuuki and Y. Matsui, Jpn. *J.Appl. Phys.*, **30**(3), 431 (1991).
20. G. Lucovsky and D. V. Tsu, *J. Cryst. Growth*, **86**, 804 (1988).
21. R. J. Joyce, H. F. Sterling and J. H. Alexander, *Thin Solid Films*, **1**, 481 (1967/68).
22. S. Rhee and J. Rhee, CVD Handbook, Bando Publishing Co., Seoul, p. 304 (1993).
23. W. A. Ranford, M. J. Rand, *J. App. Phys.*, **49**, 2473 (1978).
24. Yi Ma, T. Yasuda, S. Habermehl, and G. Lucovsky, *J. Vac. Sci. Technol., A*, **A10**(4), 781 (1992).
25. E. H. Poindexter, G. J. Geradi, M. E. Rueckel, and P. J. Caplan, *J. Appl. Phys.*, **56**, 2884 (1984).